A New Family of Sequence-Specific DNA-Cleaving Agents Directed by Triple-Helical Structures: Benzopyridoindole – EDTA Conjugates

Christophe Marchand,[a] Chi Hung Nguyen,[b] Brian Ward,[c] Jian-Sheng Sun,*[a] Emile Bisagni,[b] Thérèse Garestier,[a] and Claude Hélène[a]

Abstract: Sequence-specific DNA recognition can be achieved by oligonucleotides that bind to the major groove of oligopyrimidine·oligopurine sequences. These intermolecular structures could be used to modulate gene expression and to create new tools for molecular biology. Here we report the synthesis and biochemical characterization of triple helix-specific DNA cleaving reagents. It is based on the previously reported triplex-specific ligands, benzo[e]pyridoindole (BePI) and benzo[g]-pyridoindole (BgPI), covalently attached to ethylenediaminotetraacetic acid (EDTA). In the presence of iron, a reducing agent and molecular oxygen, BgPI – EDTA·Fe^{II} but not BePI – EDTA·Fe^{II} induced a double-stranded cut in a plasmid DNA at the single site where a triplex-forming oligonucleotide binds. At single nucleotide resolution, it was found that upon triplex formation BePI – EDTA·Fe^{II} led to cleavage of the pyrimidine strand and protection of the purine strand. BgPI – EDTA·Fe^{II} cleaved both strands with similar efficiency. The difference in cleavage efficiency between the two conjugates was rationalized by the location of the EDTA·Fe^{II} moiety with respect to the grooves of DNA (major groove: BePI – EDTA·Fe^{II}, minor groove: BgPI – EDTA·Fe^{II}). This work paves the way to the development of a new class of triple helix directed DNA cleaving reagents. Such molecules will be of interest for sequence-specific DNA cleavage and for investigating triple-helical structures, such as H-DNA, which could play an important role in the control of gene expression in vivo.

Keywords: DNA cleavage · EDTA · oligonucleotides · triple helix

Introduction

Nucleic acid triple helix formation was first observed with polyribonucleotides in 1957[1] and studied in the 60s and early 70s. In the mid-80s, it was demonstrated that: i) Intramolecular triple helices (H-DNA) may occur at mirror symmetry-related oligopyrimidine·oligopurine sequences under negative supercoiling stress[2] and ii) intermolecular triple helices can be formed at specific DNA sites using oligodeoxynucleotides.[3] As a result of these works, triple-helical structures have been the focus of intense research efforts because of their applications as molecular biology tools[4] and for the potential development of gene targeted oligonucleotide-based therapeutics.

The interactions between DNA triple helices and small ligands have been investigated in recent years. These studies were originally motivated by the desire to further stabilize DNA triplexes to improve the potential efficiency of triplex-forming oligonucleotides (TFOs) as therapeutic agents. Ethidium bromide was shown to stabilize triplexes made of T·A × T base triplets,[5, 6] and intercalate at the duplex – triplex junction.[6, 7] However, ethidium bromide destabilized triple helices containing both T·A × T and C·G × C+ base triplets.[7] The first ligands capable of preferential stabilization of T·A × T and C·G × C+ base triplets (as compared with the corresponding duplexes) were derivatives of benzo[e]pyridoindole (BePI) and benzo[g]pyridoindole (BgPI).[8] These ligands were shown to bind triple-helical structures by intercalation.[8–10]

To create a new family of triple helix specific DNA cleaving agents, we linked an EDTA moiety to BePI and BgPI through their aminoalkyl side chains (Figure 1). In the presence of iron, a reducing agent and molecular oxygen, EDTA·Fe^{II} complexes generate OH· radicals, according to the Fenton reaction, which leads to DNA strand scission by attack of the

[a] Prof. Dr. J.-S. Sun, Dr. C. Marchand, Prof. Dr. T. Garestier, Prof. Dr. C. Hélène
Laboratoire de Biophysique
UMR8646 CNRS-Muséum National d'Histoire Naturelle
INSERM U201
43 rue Cuvier, 75231 Paris cedex 05 (France)
Fax: (+33) 1-40793705
E-mail: sun@mnhn.fr

[b] Dr. C. H. Nguyen, Dr. E. Bisagni
UMR176 CNRS-Institut Curie, Section Recherche
15 rue Georges Clémenceau, 91405 Orsay (France)

[c] Dr. B. Ward
Sigma Chemical Company
P.O. Box 14508, Saint Louis, MO 63178 (USA)

  0947-6539/00/0609-1559 $ 17.50+.50/0

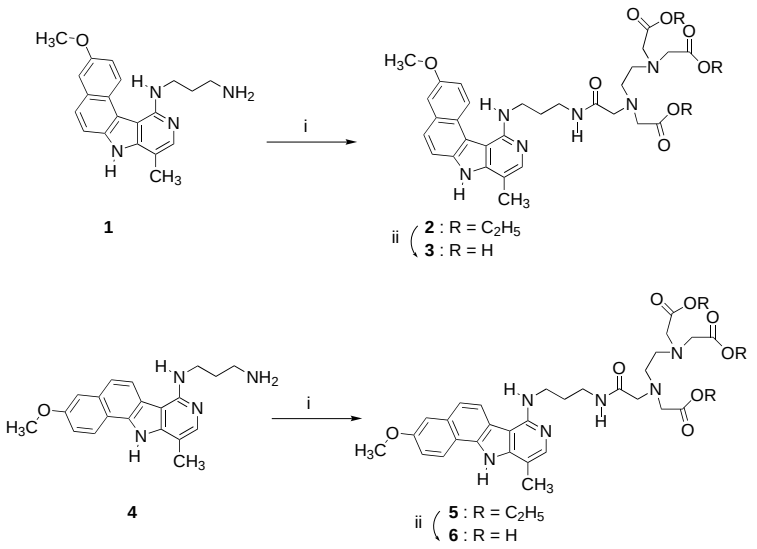

Figure 1. Synthesis of BePI–EDTA (compound **3**) and BgPI–EDTA (compound **6**). i) EDTA-TEE, EDCI, CH_2Cl_2/MeOH, 20 °C, 48 h (52–60 %); ii) a) LiOH, MeOH/H_2O, 0 °C, 48 h; b) HCl (66–82 %).

deoxyribose moiety in the minor groove of duplex DNA.[11, 12] Covalent attachment of the EDTA moiety to a triplex-specific ligand was expected to target cleavage to triple helix sites.

Results and Discussion

Chemistry: BPI–EDTAs were synthesized in good overall yield according to the reaction schemes outlined in Figure 1. Condensation between EDTA triethyl ester and the BPI aminoalkyl side chains was mediated by 1-(3-dimethylaminopropyl)-3-ethylcarbodiimide (EDCI). Base hydrolysis of BPI–EDTA triethyl esters afforded BPI–EDTAs (see Experimental Section for details).

Triple helix directed cleavage on a plasmid DNA: Comparative triplex-directed double strand DNA cleavage by BgPI- and BePI–EDTA·Fe^{II} was investigated using a linearized (*Sca*I, position 2222, Figure 2) plasmid DNA (pA20) engineered to contain a dT_{20}·dA_{20} tract for binding the simple TFO dT_{20}.[13] Triplex-directed specific cleavage of the linear plasmid should produce two series of fragments centered at 953- and 1775-bp. Since the TFO binding site (position 437–457) was introduced into the multiple cloning site of pUC19, these fragments will migrate on a low percentage agarose gel with an electrophoretic mobility that is similar to *Eco*RI (position 397). While either molecule was able to inflict much concentration-dependent duplex DNA damage (Figure 2, non-specific cleavage products lanes 5–9 and 14–18), only BgPI–EDTA·Fe^{II} was able to specifically produce double-stranded cleavage products at the TFO's target site, as evidenced by the expected fragments (Figure 2, lanes 5–9) that nearly co-migrate with the cleavage products from an *Eco*RI partial digest (Figure 2, lane 2). At 20 μM dT_{20}, specific cleavage of *Sca*I pA20 by BgPI–EDTA·Fe^{II} was dose-dependent from above 1 to approximately 25 μM. Above 25 μM, non-specific cleavage continued to be dose-dependent while specific cleavage reached a steady state (i.e., was dose-independent). In the presence of a non-binding oligopyrimidine (25 μM $d(TC)_{10}$), only non-specific cleavage was observed (data not shown). We investigated DNA cleavage by both compounds at single nucleotide resolution to understand the discrepancy between triplex-specific cleavage yet triplex stabilization by the two molecules.

Single nucleotide resolution of triple helix directed DNA cleavage: A ^{32}P 5′-end labeled 80-bp DNA fragment containing a 27-bp oligopyrimidine·oligopurine tract was used as a target for triplex formation by a 27-nt TFO (Figure 3) to characterize triplex-specific cleavage by BPI–EDTA·Fe^{II}. For reference, the free and TFO bound fragment was cut using methidiumpropyl EDTA (MPE).[14] Examination of the autoradiogram (Figure 3)

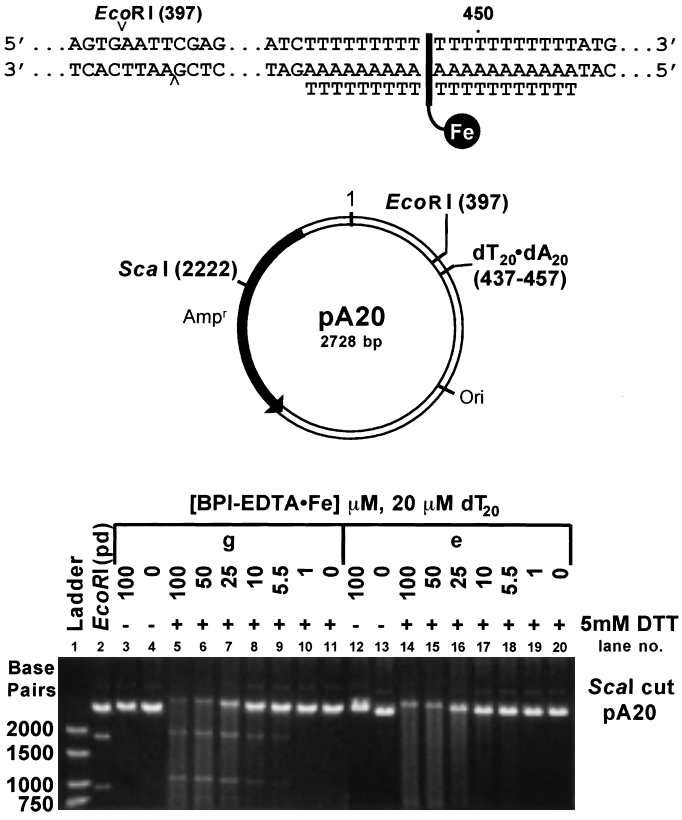

Figure 2. Top: Map of pA20. The expanded sequence shows a cartoon of the engineered sequence with the third strand and BPI–EDTA·Fe^{II} bound. Amp^r indicates the ampicillin-resistant gene, Ori is the origin of replication. Bottom: Cleavage of linearized pA20 plasmid DNA by BPI–EDTA·Fe^{II}. *Eco*RI(pd) is a partial digest of linearized pA20. Lanes marked (−) and (+) are without or with 5 mM DTT initiation, respectively; lanes g and e are treated with BgPI–EDTA·Fe^{II} and BePI–EDTA·Fe^{II}, respectively. The concentration of the reagent (μM) is indicated above the lanes. The concentration of dT_{20} was 20 μM in all reactions.

0947-6539/00/0609-1560 $ 17.50+.50/0 *Chem. Eur. J.* **2000**, *6*, No. 9

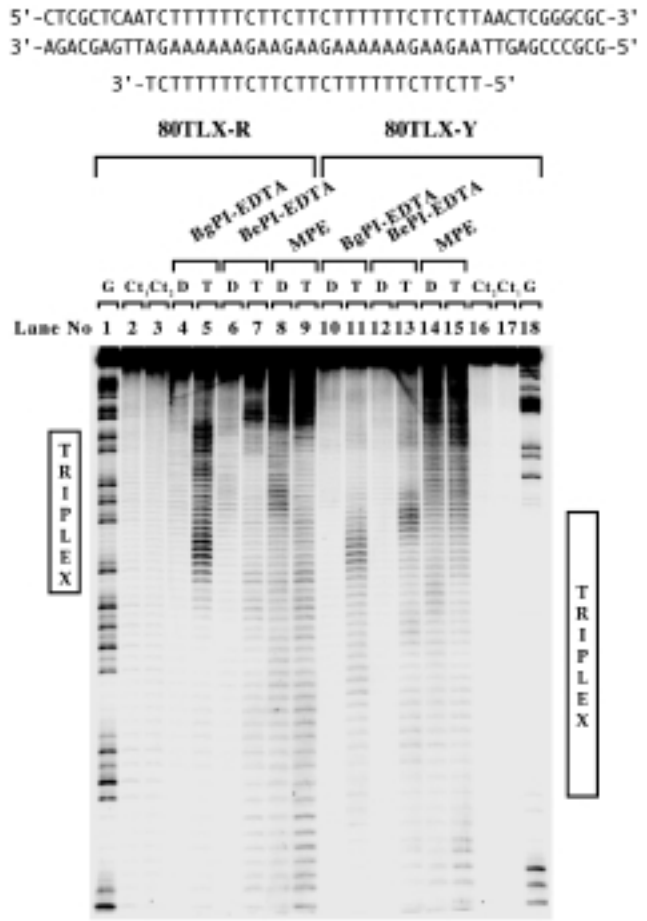

Figure 3. The 27-bp oligopyrimidine·oligopurine sequence in the 80TLX DNA fragment and TFO used in this work (top). Reaction of the 80TLX DNA fragment labeled at the 5′-end on the oligopurine-containing strand (80TLX-R) or on the oligopyrimidine-containing strand (80TLX-Y) with 20 μM of BgPI–EDTA, BePI–EDTA and MPE in the presence of specific third strand (T) or non-relevant third strand (D). Two controls were included: DNA + Fe^{II} (Ct1) and DNA + Fe^{II} + DTT (Ct2). Triple helix sites are indicated. G lanes (1 and 18) are Maxam Gilbert sequencing of guanines using DMS treatment.

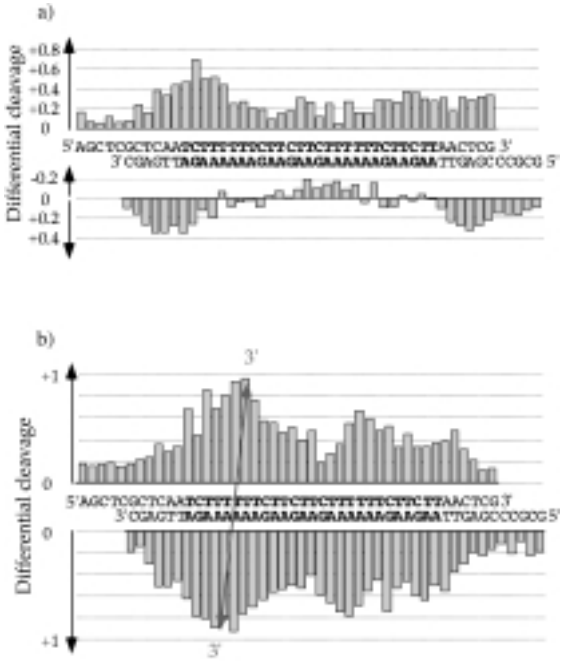

Figure 4. Differential cleavage plots comparing BePI–EDTA·Fe^{II} a) and BgPI–EDTA·Fe^{II}-mediated cleavage b) on the 80TLX DNA fragment. The plots were obtained by taking the logarithm of the ratio of the triplex (T) and duplex (D) band densities at each nucleotide. Positive and negative values correspond, respectively, to enhanced or decreased cutting efficiency in the triplex.

reveals that: i) at identical concentrations (20 μM), the triplex specific cleavage reagents cleaved duplex DNA less efficiently than MPE (lanes 4 and 6 versus 8; lanes 10 and 12 versus 14); ii) triplex formation protects the TFO binding site from cleavage by MPE (lanes 8 versus 9 and 14 versus 15), providing conclusive evidence that the TFO was bound to target under the experimental conditions; iii) triplex formation induced enhanced cleavage by BgPI- and BePI–EDTA·Fe^{II} conjugates. Consistent with the linearized plasmid results, differential densitometric analysis (Figure 4) shows that strong DNA cutting was promoted by BgPI–EDTA conjugate on both strands within the triplex site. For BePI–EDTA, enhanced cleavage on the pyrimidine strand and a protection/footprint on the oligopurine-containing strand was observed.

The most intense cleavage sites of the TFO-bound duplex by BgPI–EDTA·Fe^{II} are centered around the preferred benzopyridoindole (BPI) binding sites[15] (i.e., $T_6 \cdot A_6$). Close inspection of the distribution of cleavage reveals that the peaks of cleavage are displaced to 3′ end on both strands by two base pairs. This displacement is also observed at the TFO's 3′ end using BePI–EDTA·Fe^{II}. 3′ displacement indicates that a DNA cleaving reagent is localized in minor groove. This is also consistent with diffusive HO· radicals generated by EDTA·Fe^{II} which induces DNA strand cleavage by attacking deoxyriboses from the minor groove by H4′/H1′ abstraction.

The observed difference in the pattern and efficiency with which BgPI- and BePI–EDTA·Fe^{II} cleave DNA can be explained by the location of EDTA·Fe^{II} complex. We previously showed that the aminoalkyl side chain of BgPI derivatives was located in the minor groove of both duplexes and triplexes (Figure 5, top left). For BePI, the side chain was in the Watson–Hoogsteen (major) groove (Figure 5, top right),[15, 16] whereas it was located in the minor groove of duplex.[9] Because the EDTA moiety was covalently attached to BPI derivatives via an amide bond through the aminoalkyl side chain, we expected the EDTA·Fe^{II} moiety (warhead) to be in the minor groove for BgPI–EDTA and the major groove for BePI–EDTA in triplex. The relative triplex-specific cutting efficiency of BgPI- versus BePI–EDTA·Fe^{II} is consistent with this expectation. The proximal location of EDTA·Fe^{II} moiety in BgPI–EDTA near the H4′/H1′ hydrogen led to efficient scission of both strands by free radicals (Figure 5, bottom). In contrast, hydroxyl radicals generated by BePI–EDTA·Fe^{II} must diffuse from the major to the minor groove, the strand scission was therefore less efficient. Actually, triplex-specific cleavage was observed on the more proximal, that is oligopyrimidine-containing, Watson-Crick strand. The more distant oligopurine-containing strand was even protected from strand scission upon triplex formation. It is unlikely that this is due to a TFO-induced conformational

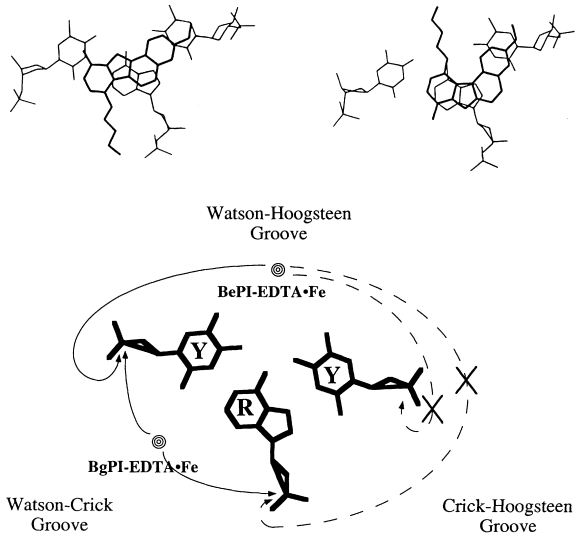

Figure 5. Top: Orientation of BgPI (left) and BePI (right) with respect to the base triplets. These pictures were taken from the previously published energy-minimized models in which both BPI molecules were intercalated in triplex (for details see [15,16]). Bottom: Schematic representation of the location of the EDTA·Fe^{II} moiety in different grooves and the accessibility of the H1′ and H4′ hydrogens for both oligopyrimidine and oligopurine-containing strands of the DNA double helix in the Watson–Crick groove and for the pyrimidine third strand in the Crick–Hoogsteen groove.

change to the duplex, which might have changed the accessibility/reactivity of the deoxyribose protons. It seems that conformational change in the minor groove upon triplex formation was not enough to be revealed by hydroxyl radical footprint.[17] Therefore the observation that the purine strand in triplex is protected relative to the duplex can be rationalized by the expected position of the warhead in triplex BePI–EDTA·Fe^{II} complexes versus the same complex in duplex. An increase in cleavage efficiency of the oligopyrimidine-containing strand is likely a result of tighter ligand binding to triplex than duplex. An increased cleavage of the oligopurine-containing strand by BePI–EDTA·Fe^{II} at the duplex/triplex junctions could also be rationalized by tighter binding of the intercalator at the duplex–triplex junction and the minor groove location of the warhead at the junction.

No notable third strand cleavage was observed by either BPI–EDTA·Fe^{II} complex using a labeled third strand oligonucleotide (data not shown). Inspection on a triplex model shows that the H4′/H1′ hydrogens on the third strand are deeply buried in the narrow Crick–Hoogsteen groove and not easily accessible to diffusible radicals. It would be interesting to investigate cleavage using triplex specific intercalators that placed the warhead at point blank range of the H4′/H1′ hydrogens in the third strand.

Considerations for designing triplex-specific cleaving agents:

$$\text{Triplex} + \text{TSI–EDTA}\cdot Fe^{II} \overset{K_T}{\rightleftharpoons} (\text{Triplex-TSI-EDTA}\cdot Fe^{II}) \xrightarrow{k_T} \text{Cut Triplex (duplex)}$$

versus

$$\text{Duplex} + \text{TSI–EDTA}\cdot Fe^{II} \overset{K_D}{\rightleftharpoons} (\text{Duplex-TSI-EDTA}\cdot Fe^{II}) \xrightarrow{k_D} \text{Cut Duplex}$$

Designing cleaving reagents that effectively cut triplex but not duplex DNA requires addressing the reaction from two fronts. The first is the selectivity of the structure-specific binding agent (e.g., the triplex-specific intercalator, TSI) and the second is the efficiency of strand scission. The reactions to be considered are given in the scheme above: K_T and K_D are the association equilibrium constants for structure recognition, k_T and k_D are rate constants for the cleavage of triplex and duplex, respectively. In this work we have demonstrated that k_T is critically dependent upon the placement of the warhead on the intercalative macrocycle which determines the location of the warhead with respect to the grooves in the triplex structure ($k_T^{\text{BgPI–EDTA·iron(II)}} \gg k_T^{\text{BePI–EDTA·iron(II)}}$). Thus, for efficient cleavage the radical source should be within close range of the target hydrogen atom. Assuming future triplex-specific DNA cleaver can be designed to place the warhead within the closest proximity of H4′/H1′ hydrogens in Watson–Crick strands, maximum selectivity will be governed by the ability of the TSI to distinguish triplex from duplex. As the reverse was demonstrated with BePI–EDTA·Fe^{II}, selectivity could be further enhanced using TSIs whose side chains reside in the major groove when bound to duplex yet minor groove when triplex bound. Thus, maximal selectivity could be accomplished using intercalators whose K_T and k_T are very much larger than K_D and k_D, respectively. Second generation cleavage reagents are now being investigated in our laboratories using more highly selective TSIs (e.g., benzoindoloquinoline[16] and benzoquinoquinoxaline[18]).

In the literature, triple helix directed DNA cleavage has been achieved by attaching an EDTA moiety to TFO.[3b] It was shown that the reaction was highly selective to a single site in an engineered strain of yeast due to sequence-specific triple helix formation, but the cleavage yield was quite low (about 6% after two repeated treatments).[22] The low dsDNA cleaving yield could also be explained by the major groove location of the EDTA·Fe^{II} warhead since the EDTA was tethered to the C5 atom of thymine. The improved TSI–EDTA compounds should be more efficient to cleave DNA than TFO–EDTA conjugate, however it remains to demonstrate that they can be as selective as the TFO–EDTA molecules. If so, the TSI–EDTA molecules would be a versatile triple-helical structure cleaving agents, and therefore, could be used to probe naturally occurring triple-helical structures.

Conclusion

The present work shows that the concept of attaching a reactive warhead to a triplex-specific ligand to create triplex-specific DNA probes was validated. This proof-of-principle work shows also that the localization of the EDTA·Fe^{II} moiety is very important to ensure efficient DNA cleavage. The radical source should be in close proximity to the target deoxyribose for maximal efficiency. Triple helical structure directed DNA cutting agents will be useful for probing unusual DNA structures such as H-DNA. Because BPI derivatives stabilize RNA structures,[19] triplex cleavage agents could also be used to map folded RNA structures that

0947-6539/00/0609-1562 $ 17.50+.50/0 *Chem. Eur. J.* **2000**, *6*, No. 9

involve base triplets. These structural identifications will add to our understanding of the biological roles that triple helices play in vivo. Second generation studies, using highly specific intercalators, are in progress in our laboratories to develop highly efficient triplex structural probes.

Experimental Section

Oligonucleotides: Oligonucleotides (OligoGold grade) were synthesized by Eurogentec (Seraing, Belgium), and were used after ethanol precipitation.

Chemicals: BePI (**1**) and BgPI (**4**) (Figure 1) were prepared as previously described.[20, 21] Methidiumpropyl EDTA (MPE), ethylenediaminetetraacetic acid triethyl ester hydrochloride (EDTA-TEE) and 1-(3-dimethylaminopropyl)-3-ethylcarbodiimide (EDCI) were purchased from Sigma Co. and Aldrich Co., respectively. Melting points (M.p., uncorrected) were measured using an Electrothermal IA9200 melting point apparatus. ^{1}H-NMR spectroscopy was performed on a Bruker AC200 spectrometer in [D_6]DMSO in the presence of a drop of D_2O as solvents and ^{1}H chemical shifts were referenced to residual DMSO peak ($\delta = 2.54$). Elemental analysis was performed by Service Central de microanalyses du CNRS, 91190 Gif-sur-Yvette, France. The results are within ± 0.4% of the theoretical values corresponding to the mentionned empirical formula.

Synthesis of BePI–EDTA (Compound 3): EDTA-TEE hydrochloride (500 mg, 1.16 mmol) was dissolved in water (10 mL) and 1 equiv NaOH was added at 0 °C. After extraction with CH_2Cl_2 (4 × 20 mL), the organic layers were dried over $MgSO_4$ and evaporated to dryness. The free base of EDTA-TEE thus obtained (200 mg, 0.53 mmol) was dissolved in CH_2Cl_2/MeOH (1:1, 4 mL) and after addition of BePI **1** (133 mg, 0.4 mmol) in MeOH (8 mL) and EDCI (132 mg), the mixture was kept at room temperature for 48 h. The intermediate BePI–EDTA triethyl ester **2** (145 mg, 52% yield) was obtained after solvent removal under reduced pressure and flash chromatography on silica gel (h = 45 cm, $\phi = 2.2$ cm) using a gradient of ethanol (0–3%) in CH_2Cl_2. Compound **2** (145 mg, 0.20 mmol), dissolved in MeOH (6 mL), was added at 0 °C to a mixture of MeOH/H_2O (1:1, 6 mL) containing LiOH hydrate (50 mg, 1.2 mmol). After 48 h at 0 °C, the pH was adjusted to ca. 4 with 1 M HCl and then neutralized with 28% NH_4OH/MeOH 1:9. Evaporation to dryness followed by chromatography on silica gel (h = 45 cm, $\phi = 2.2$ cm) using a gradient (0.1–0.3%) of 28% NH_4OH in MeOH gave colorless microcrystals of BePI–EDTA (110 mg, 82%). M.p: 225–226 °C; ^{1}H NMR (25 °C): $\delta = 8.8$ (d, ^3J(H,H) = 9.2 Hz, 1H; Ar-H), 8.1 (s, 1H; Ar-H), 8.0 (d, ^3J(H,H) = 9.2 Hz, 1H; Ar-H), 7.8 (d, ^3J(H,H) = 8.8 Hz, 1H; Ar-H), 7.6 (s, 1H; Ar-H), 7.4 (d, ^3J(H,H) = 8.8 Hz, 1H; Ar-H), 3.9 (s, 3H; CH_3), 3.7 (m, 2H; CH_2), 3.6–3.3 (m, 12H; 6CH_2), 3.1 (m, 2H; CH_2), 2.5 (s, 3H; CH_3), 2.0 (m, 2H; CH_2); $C_{30}H_{36}N_6O_8 \cdot 2H_2O$ (644.7): calcd C 55.89, H 6.25, N 13.04, O 24.82; found C 55.50, H 6.14, N 12.89, O 25.16.

Synthesis of BgPI–EDTA (Compound 6): As with compound **3** (above), compound **6** was prepared starting from BgPI **4** via the preparation and hydrolysis of BgPI–EDTA-TEE **5** (60%). Hydrolysis of **5** gave BgPI–EDTA **6** (66%). M.p: 219–220 °C; ^{1}H NMR (25 °C): $\delta = 8.7$ (d, ^3J(H,H) = 8.9 Hz, 1H; Ar-H), 8.6 (d, ^3J(H,H) = 8.5 Hz, 1H; Ar-H), 7.9 (s, 1H; Ar-H), 7.7 (d, ^3J(H,H) = 8.5 Hz, 1H; Ar-H), 7.5 (s, 1H, Ar-H), 7.4 (d, ^3J(H,H) = 8.9 Hz, 1H; Ar-H), 3.9 (s, 3H; CH_3), 3.7–1.8 (m, 21H; 9CH_2+CH_3); $C_{30}H_{36}N_6O_8 \cdot 4H_2O$ (680.7): calcd C 52.93, H 6.52, N 12.35, O 28.20; found C 53.11, H 6.13, N 12.52, O 28.43.

Plasmid DNA cleavage assay: Plasmid DNA (pA20) was prepared as previously described.[13] *Sca*I cleavage of pA20 (position 2222) was accomplished by cleaving 80 μg of plasmid with 2500 units of *Sca*I (NEB) at 37 °C overnight. Specific cleavage (positions 437–457) was verified by co-migration analysis with *Eco*RI (position 396) cut *Sca*I-pA20 and a commercial molecular weight marker (Sigma). BgPI- or BePI–EDTA solutions were prepared in DMSO (Sigma) and concentrations were determined using published extinction coefficients).[9] All cleavage reactions were pre-equilibrated in 10 mM cacodylate buffer (pH 7.0), 100 mM NaCl overnight at 25 °C. Reactions were initiated by addition of 20 μM $Fe(NH_4)_2(SO_4)_2$ and 5 mM dithiothreitol (DTT). Reactions were terminated by addition of gel loading solution (Sigma) followed immediately by 1% agarose gel electrophoresis.

Cleavage assay on an 80-bp DNA fragment: A 80-bp fragment was prepared after digestion of plasmid pLTX (a gift from Dr. Christian Bailly) by restriction enzyme *Eco*RI and *Hin*dIII. This fragment contains a 27-bp oligopyrimidine·oligopurine sequence (Figure 3, top). The oligopurine- and oligopyrimidine-containing strands of the 80-bp DNA fragment were separately 5′-end radiolabeled (R*Y or Y*R) by T4 polynucleotide kinase (Biolabs). Samples of this fragment were incubated one hour at room temperature in 10 mM cacodylate buffer (pH 6.0), 50 mM NaCl and 10 mM $MgCl_2$ in the presence of 20 μM non-specific d(GGGTTTTTTTTGGGTTTGGGTTGGGG) or d(TC)$_{13}$T, or in the presence of 20 μM specific d(TTCTTCTTTTTTCTTCTTCTTTTTTCT) oligonucleotide, in the presence of 20 μM BPI–EDTA or MPE, respectively. 20 μM $Fe(NH_4)_2(SO_4)_2$ was then added to each sample. Cleavage reaction was triggered by adding 5 mM dithiothreitol and carried out for 15 min at room temperature. The reaction was stopped by ethanol precipitation and loaded on an acrylamide gel for analysis.

Acknowledgement

The authors thank Dr. Christian Bailly for providing pLTX plasmid containing the 27-bp oligopyrimidine·oligopurine sequence, and Terry Petronzio at NEB for assistance with *Sca*I plasmid digest conditions. This work was supported by "Action Concertée et Coordonée" programme (CNRS). C.M. was supported by a Ph.D training grant of "Ministère de la Recherche et de l'Enseignement".

[1] G. Felsenfeld, D. R. Davies, A. Rich, *J. Am. Chem. Soc.* **1957**, *79*, 2023–2024.
[2] S. M. Mirkin, V. I. Lyamichev, K. N. Drushlyak, V. N. Dobrynin, S. A. Filippov, M. D. Frank-Kamenetskii, *Nature* **1987**, *330*, 495–498.
[3] a) T. Le Doan, L. Perrouault, D. Praseuth, N. Habhoub, J. L. Decout, N. T. Thuong, J. Lhomme, C. Hélène, *Nucleic Acids Res.* **1987**, *15*, 7749–7760; b) H. E. Moser, P. B. Dervan, *Science* **1987**, *238*, 645–650.
[4] N. T. Thuong, C. Hélène, *Angew. Chem.* **1993**, *105*, 697–723; *Angew. Chem. Int. Ed. Engl.* **1993**, *32*, 666–690.
[5] P. V. Scaria, R. H. Shafer, *J. Biol. Chem.* **1991**, *266*, 5417–5423.
[6] J. L. Mergny, D. Collier, M. Rougée, T. Montenay-Garestier, C. Hélène, *Nucleic Acids Res.* **1991**, *19*, 1521–1526.
[7] J. S. Sun, R. Lavery, J. Chomilier, K. Zakrzewska, T. Montenay-Garestier, C. Hélène, *J. Biomol. Struct. Dyn.* **1991**, *9*, 425–436.
[8] J. L. Mergny, G. Duval-Valentin, C. H. Nguyen, L. Perrouault, B. Faucon, M. Rougée, T. Montenay-Garestier, E. Bisagni, C. Hélène, *Science* **1992**, *256*, 1681–1684.
[9] D. S. Pilch, M. J. Waring, J. S. Sun, M. Rougée, C. H. Nguyen, E. Bisagni, T. Garestier, C. Hélène, *J. Mol. Biol.* **1993**, *232*, 926–946.
[10] S. K. Kim, J. S. Sun, T. Garestier, C. Hélène, C. H. Nguyen, E. Bisagni, A. Rodger, B. Norden, *Biopolymers* **1997** *42*, 101–111.
[11] G. E. Shafer, T. D. Tulluis, *Electrophoresis* **1989**, *10*, 397–404.
[12] T. D. Tulluis, *Free Radic. Res. Commun.* **1991**, *12*, 251–259.
[13] B. Ward, *Nucleic Acids Res.* **1996**, *24*, 2435–2440.
[14] R. P. Hertzberg, P. B. Dervan, *Biochemistry* **1984**, *23*, 3934–3945.
[15] C. Escudé, C. H. Nguyen, J. L. Mergny, J. S. Sun, E. Bisagni, T. Garestier, C. Hélène, *J. Am. Chem. Soc.* **1995**, *117*, 10212–10219.
[16] C. H. Nguyen, C. Marchand, S. Delage, J. S. Sun, T. Garestier, C. Hélène, E. Bisagni, *J. Am. Chem. Soc.* **1998**, *120*, 2501–2507.
[17] K. Fox, personal communication.
[18] C. Escudé, C. H. Nguyen, S. Kukreti, Y. Janin, J. S. Sun, E. Bisagni, T. Garestier, C. Hélène, *Proc. Natl. Acad. Sci. USA* **1998**, *95*, 3591–3596.
[19] C. Escudé, personal communication.
[20] C. H. Nguyen, F. Lavelle, J. F. Rio, M. C. Bisserey, C. Huel, E. Bisagni, *Anti-Cancer Drug Des.* **1992**, *7*, 235–251.
[21] C. Escudé, C. H. Nguyen, J. L. Mergny, J. S. Sun, E. Bisagni, T. Garestier, C. Hélène, *J. Am. Chem. Soc.* **1995**, *117*, 10212–10219.
[22] S. A. Strobel, P. B. Dervan, *Science* **1990**, *249*, 73–75.

Received: July 12, 1999 [F1907]